Journal of
Applied Remote Sensing

RemoteSensing.SPIEDigitalLibrary.org

Performance of existing QAAs in Secchi disk depth retrieval in phytoplankton and dissolved organic matter dominated inland waters

Thanan Rodrigues
Enner Alcântara
Deepak R. Mishra
Fernanda Watanabe
Nariane Bernardo
Luiz Rotta
Nilton Imai
Ike Astuti

SPIE.

Thanan Rodrigues, Enner Alcântara, Deepak R. Mishra, Fernanda Watanabe, Nariane Bernardo, Luiz Rotta, Nilton Imai, Ike Astuti, "Performance of existing QAAs in Secchi disk depth retrieval in phytoplankton and dissolved organic matter dominated inland waters," *J. Appl. Remote Sens.* **12**(3), 036017 (2018), doi: 10.1117/1.JRS.12.036017.

Performance of existing QAAs in Secchi disk depth retrieval in phytoplankton and dissolved organic matter dominated inland waters

Thanan Rodrigues,[a,*] Enner Alcântara,[b] Deepak R. Mishra,[c] Fernanda Watanabe,[d] Nariane Bernardo,[d] Luiz Rotta,[d] Nilton Imai,[d] and Ike Astuti[e]

[a]Federal Institute of Education, Science and Technology of Pará State, Castanhal, Brazil
[b]São Paulo State University, Department of Environmental Engineering, São José dos Campos, Brazil
[c]University of Georgia, Department of Geography, Athens, United States
[d]São Paulo State University, Department of Cartography, Presidente Prudente, Brazil
[e]State University of Malang, Department of Geography, Semarang, Indonesia

Abstract. A semianalytical model developed to estimate the Secchi disk depth (Z_{SD}) was used in eutrophic-to-hypereutrophic reservoirs (Ibitinga, Ibi, and Barra Bonita, BB) placed in the cascade system of the Tietê River, Brazil. The model was evaluated using the simulated remote sensing reflectance based on the Ocean and Land Color Instrument/Sentinel-3A and the Operational Land Imager/Landsat-8 from both reservoirs. Three quasianalytical algorithm (QAA) versions (QAA_{v5}, QAA_{M14}, and QAA_{W16}) were evaluated to derive the absorption and backscattering coefficients, and then used for Z_{SD} retrieval. For BB, where the chlorophyll-*a* concentration exceeded 200 mg m^{-3}, the model based on QAA_{v5} showed high uncertainties while the QAA_{W16}, which was originally parameterized for BB showed better performance regarding the Z_{SD} retrieval (mean absolute percentage errors—MAPE of 22%). However, QAA_{W16} did not perform satisfactorily for Ibi, which is dominated by colored dissolved organic matter (CDOM). For Ibi, QAA_{v5} provided the best result with MAPE of 34.60%, followed by QAA_{M14} with 34.65%. QAA-based Z_{SD} models tend to perform poorly in waters with high concentration of chlorophyll-*a* possibly due to phytoplankton package effect, whereas the same models may require additional parameterization in waters dominated by CDOM. Landsat-8 data showed significant potential for Z_{SD} retrieval in inland waters. [DOI: 10.1117/1.JRS.12.036017]

Keywords: water quality; remote sensing; inland waters; bio-optical model.

Paper 180327L received Apr. 18, 2018; accepted for publication Aug. 15, 2018; published online Sep. 12, 2018.

1 Introduction

Water transparency is often related to water quality since it shows the impact of in-water components to the attenuation of light. Secchi disk depth (Z_{SD}), a proxy for water clarity, can be useful to estimate the concentrations of phytoplankton or suspended matter and to evaluate the trophic status and need for restoration of a water body.[1] Collecting representative *in situ* Z_{SD} for a water body is both labor and cost intensive and not practical, therefore demands a remote sensing solution that could be very useful in water quality monitoring.

Satellite remote sensing has been used frequently for estimating optically significant constituents such as chlorophyll-a (Chl-a), suspended particulate matter (SPM), and colored dissolved organic matter (CDOM), particularly in ocean and coastal waters. To retrieve Z_{SD} from space, authors of Ref. 2 developed a new theoretical semianalytical model, which can

*Address all correspondence to: Thanan Rodrigues, E-mail: thanan.rodrigues@ifpa.edu.br

1931-3195/2018/$25.00 © 2018 SPIE

Table 1 Summary of QAA versions applied to turbid inland waters and their performances to derive $a(\lambda)$.

QAA version (λ_0)	Water type	Accuracy	Sensor center bands (nm)
QAA_Turbid (753 nm)[5]	Asian lakes	$0.075 < \text{RMSE}_{\text{log}}$[a] < 0.130	MERIS (413 to 665)
QAA_{M14} (708 nm)[7]	Aquaculture ponds	Average $\varepsilon(\lambda) = 19.87\%$[b]	MERIS (413 to 665)
QAA_{W16} (709 nm)[8]	Eutrophic reservoir	Average MAPE $= 28.27\%$[c]	MERIS (413 to 709)
QAA_{OMW} (709 nm)[9]	Oligomesotrophic reservoir	Average MAPE $= 16.35\%$	OLCI (412 to 709)

[a]RMSE_{log}, root mean square error in log scale.
[b]ε, linear percentage error.
[c]MAPE, mean absolute percentage error.

be applicable to a wide range of environments. However, the approach did not consider very turbid and productive waters, where the absorption and scattering components are higher, making the water body optically more complex than coastal and seawaters.[3]

The estimation of the inherent optical properties (IOPs) represented by the total absorption and backscattering coefficients [$a(\lambda)$ and $b_b(\lambda)$], used as input for the model from Ref. 2 was based on the quasianalytical algorithm (QAA[4]), which was also designed for ocean and coastal waters; however, for turbid inland waters, authors of Refs. 5 and 6 observed that reparameterizing the native form of QAA significantly improved the accuracy of estimation of the vertical diffuse attenuation coefficient (K_d) and the euphotic zone depth (Z_{eu}). For that reason, the native form of QAA[2] performed poorly in retrieving the Z_{SD} in two eutrophic reservoirs placed in a cascade system in Brazil. The first one (upstream) is Barra Bonita (BB), which is dominated by phytoplankton, and the other (downstream) is Ibitinga (Ibi), a dissolved organic matter dominated system.

Observing the main QAA versions available for inland waters, it is noticeable that shifting the reference wavelength (λ_0) to the near-infrared, the retrieval of $a(\lambda)$ gets improved. Several researches reparameterized the original form of QAA[4] and modified the empirical steps regarding the estimation of $a(\lambda)$ and $b_b(\lambda)$ and obtained the results presented in Table 1.

The main issues regarding the application of the original QAA in turbid inland waters were listed by Ref. 5, and it was related to the λ_0 chosen to derive $a(\lambda)$ using a synthetic data set. An empirical step of the native form was also calibrated using data from open ocean or coastal areas, which the optical properties are different from those of the turbid inland waters.

In this study, the new theoretical semianalytical model was applied to both reservoirs to retrieve Z_{SD}. Its performance was evaluated in comparison to three QAAs, the native form of QAA developed for coastal and seawaters[10] and named as QAA_{v5}; and two reparameterized QAA employed to turbid and productive waters such as Ref. 7 (QAA_{M14}) and Ref. 8 (QAA_{W16}), respectively.

2 Material and Methods

2.1 *Study Area*

BB and Ibi reservoirs are situated in the middle portion of the Tietê River, São Paulo State (Fig. 1). BB (22°31′10″S, 48°32′3″W), created by damming of the Tietê and Piracicaba Rivers began, its operation in 1963 by flooding an area of 310 km^2, with a dam length of 480 m and residence time of 90.3 days.[11] Ibi (21°45′28″S, 48°59′30″W) is a run-of-river reservoir and began its operation in 1969 by flooding an area of 114 km^2, with an average depth of 9 m and mean residence time of 21.6 days.[11]

BB reservoir is a system characterized as polymictic and hypereutrophic to eutrophic with a high content of nutrients, whose contribution leads to the development of blooms of cyanobacteria during the summer and *Bacillariophyceae* during the winter.[12] The Piracicaba and Tietê

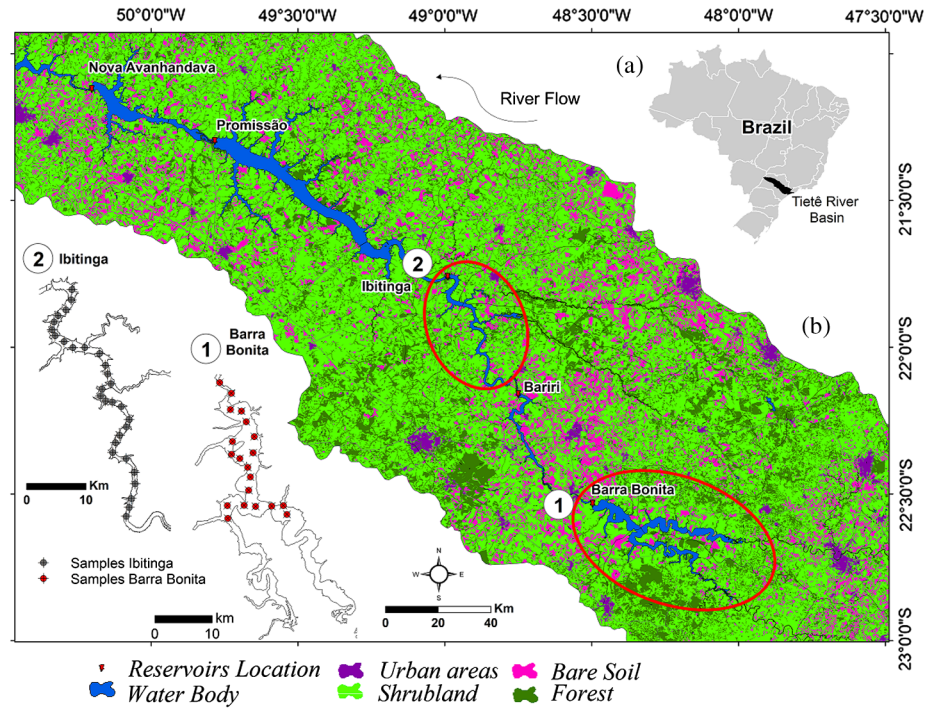

Fig. 1 Maps of study area emphasizing the (a) boundary of Brazil and the Tietê River basin, (b) land cover of Tietê River basin, and the cascade system (from upstream to downstream: BB, Bariri, Ibi, Promissão, and Nova Avanhandava); number 1 represents the sampling location of Ibitinga reservoir ($n = 30$) and number 2 ($n = 20$) depicts the sampling location of BB reservoir.

Rivers carry organic and inorganic waste from agricultural, urban, and industrial activities affecting the water quality. Ibi is characterized as polymictic, turbulent, and eutrophic reservoir; however, the trophic state can be affected by rainy and dry seasons depicting intense eutrophication process in the rainy season. The drainage basin is covered by pasture, agriculture, reforested areas, and native vegetation.

2.2 *Fieldwork*

Three field campaigns were carried out: in austral autumn (BB1: 5 to 9 May, 2014), austral spring (BB2: 13 to 16 October, 2014), and in austral winter (Ibi: 19 to 23 July, 2016). Autumn and spring are known for intermediate precipitation amounts between summer (wet period) and winter (dry period). The samples collected near the dam ($n \sim 3$) were spectrally clearer than the others along the reservoir considering BB1. For BB2, the samples were collected in the same spots as BB1; however, all of them showed to be spectrally turbid. For Ibi, the samples were collected along the reservoir respecting a minimum distance of 1 km. The spectral variability was not evident due to homogeneous turbidity along the river.

2.3 *Biogeochemical Characterization*

Water samples were acquired from the surface layer of the water column (~20 cm) and then filtered under vacuum pressure through a Whatman fiberglass GF/F filter with a porosity of 0.7 μm, and then frozen for laboratory analysis. The chlorophyll was extracted by maceration in 90% acetone solution and analyzed by a spectrophotometer.[13] The method described in Ref. 14 was used to determine the SPM concentration, which consisted in the filtration of the water on the same day of collection through a Whatman fiberglass GF/F filter with 0.7 μm pores previously calcined at 470°C, then refrigerated until analysis. The filters were placed for 12 h in an oven at 100°C, after which they were weighed, then placed in an oven at 470°C for 1 h and, finally, weighed again.

2.4 *In Situ Radiometric Data*

The remote sensing reflectance (R_{rs}, sr^{-1}) spectra were estimated from radiometric measurements taken between 10 a.m. and 2 p.m.[15] During the field campaigns, the sky was mostly clear with only a few days of partial cloud cover. In addition, no whitecaps or foam was observed at the time of data collection. At each sampling station, below and above water surface radiometric measurements were acquired using hyperspectral radiometers, RAMSES TriOS® (TriOS, Germany), operating in the spectral range between 400 and 900 nm. The best approximation of R_{rs} values was calculated from the radiometric quantities according to Ref. 16 and described in Ref. 17.

The R_{rs} spectra were matched with satellite data by convoluting the spectral response functions of Operational Land Imager (OLI) from Landsat-8 and of Ocean and Land Color Instrument (OLCI) from Sentinel-3 bands to derive the band-weighted reflectance data as presented as[18]

$$R_{rs}^{OLI,OLCI}(\lambda_k) = \frac{\int_{\lambda_i}^{\lambda_j} S(\lambda) R_{rs}(\lambda)}{\int_{\lambda_i}^{\lambda_j} S(\lambda)}, \tag{1}$$

where $R_{rs}^{OLI,OLCI}$ is the remote sensing reflectance at OLI and OLCI spectral bands; λ_i and λ_j are the lower and upper limits of the band λ_k, respectively. $S(\lambda)$ is the spectral response function of the i'th spectral band of OLI and OLCI.[19,20]

2.5 Z_{SD} *Semianalytical Model*

The Z_{SD} retrieval has been linked to K_d and can be analytically estimated by the new theoretical model from Lee et al. as presented as

$$Z_{SD} = \frac{1}{2.5 Min(K_d^{tr})} \ln\left(\frac{|0.14 - R_{rs}^{tr}|}{0.013}\right), \tag{2}$$

where K_d^{tr} is the diffuse attenuation coefficient of downwelling irradiance of the transparent window and here represents the minimum value within the visible domain (443, 482, 560, and 665 nm). In eutrophic waters, the maximum transmission of light occurs in the green region, and this is due to the selective absorption in the blue and red spectral regions.[1] R_{rs}^{tr} represents the remote sensing reflectance at the same wavelength chosen for K_d^{tr}.

The semianalytical model uses $a(\lambda)$ and $b_b(\lambda)$, analytically retrieved from the QAA version 5, QAA_{v5}[10] as input without any reparameterization or additional calibration. However, QAA_{v5} was first applied to coastal and ocean waters, therefore, two variants of QAA reparameterized to inland waters were also evaluated aiming to assess their performances in retrieving Z_{SD} using data from both study areas (QAA_{M14} and QAA_{W16}).[7,8] The main feature that characterizes both QAA forms is the reference wavelength (λ_0) set to 709 nm, where the $a(\lambda)$ is dominated by pure water absorption considering turbid inland waters.[7] The wavelength at 709 nm can be found in OLCI bands, but other wavelengths at the near-infrared can also be chosen depending on the satellite sensor of choice. In addition, empirical steps were also modified to meet the particularities of turbid inland waters such as the aquaculture ponds in Mississippi and in a Brazilian reservoir dominated by phytoplankton and cyanobacteria.

The statistical indicators used for model validation were the total root mean square error (RMSE) and the mean absolute percentage error (MAPE) presented as

$$\mathrm{RMSE} = \sqrt{\frac{1}{n}\sum_{i=1}^{n}(x_{est,i} - x_{meas,i})^2}, \tag{3}$$

$$\mathrm{MAPE} = \frac{100\%}{n}\sum_{i=1}^{n}\left|\frac{x_{est,i} - x_{meas,i}}{x_{meas,i}}\right|, \tag{4}$$

where n is the number of samples $x_{\text{est},i}$ and $x_{\text{meas},i}$ represent the estimated and measured values, respectively.

2.6 *Validation using OLI/Landsat-8 data*

The OLI products were downloaded from the U.S. Geological Service website. The Provisional Landsat 8 Surface Reflectance (L8SR) product, which is produced using specialized software, has been applied in aquatic environments to retrieve water quality parameters.[21] *In situ* Z_{SD} data ($n = 8$) were compared with Z_{SD} retrieved by OLI data. The *in situ* data collection occurred on the same day of Landsat-8 overpass. Images from Sentinel-3 were not used due to the absence of near-coincidence overpass data.

3 Results and Discussion

3.1 *In-Water and Optical Parameters*

The difference in average turbidity between BB1 and BB2 was statistically significant (p-value < 0.05, Table 2). The same result was also observed for Chl-a and SPM concentrations. The increase of Chl-a concentration in BB2 was due to the drought effect leading to flow reduction and longer water retention time.[22] High values of Chl-a for BB revealed the eutrophic status of the water, mainly in the winter.

Ibi showed values of Chl-a, SPM, and turbidity below the averages of BB and the water transparency was higher than in BB highlighting the slight improvement of water quality in Ibi. In addition, values of a_{CDOM} from Ibi showed twofold higher than BB1, depicting the organic matter domination. According to Ref. 23, the $a_{\text{CDOM}}(440)$ showed low spatial variability in Ibi for the months of February, March, May, and July, and the highest value was noticed upstream in the confluence of Tietê and Jacaré-Pepira Rivers, which is placed in the Environmental Protection Area of Ibitinga (APA-Ibitinga). Comparing both reservoirs, BB is more turbid due to high contribution of phytoplankton, specifically data from BB2 indicated very high algal turbidity with the highest Chl-a value being 797.80 mg m^{-3}. Ibi, on the other hand, presented low concentrations of Chl-a, where the average was 21.8 mg m^{-3} and the values ranged between 1.37 and 119.04 mg m^{-3}. The absorption data from both reservoirs again depicted the influence of phytoplankton in BB; however, Ibi showed dominance of CDOM (Fig. 2).

3.2 Z_{SD} *Estimation*

The result from the mixed data using bands from OLI (BB + Ibi) showed an RMSE of 0.69 m, which is below the average derived from the mixed data acquired in the field (mean $Z_{\text{SD}} = 1.54 \pm 0.76$ m). Analyzing of the model performance for each reservoir separately, BB and Ibi showed an average error of 0.49 and 0.89 m, respectively. Results using the simulated OLCI bands revealed different model accuracies for each reservoir as presented in Table 3.

Table 2 Summary of optical and biogeochemical parameters. Data are displayed in average (standard deviation).

	Chl-a (mg m^{-3})	SPM (mg L^{-1})	Z_{SD} (m)	Turbidity (NTU)	a_{CDOM}[a] (m^{-1})	a_{ϕ}[a] (m^{-1})
Ibi	21.8 (28.4)	2.6 (1.6)	2.2 (0.4)[b]	4.3 (1.2)	1.6 (0.8)	0.4 (0.7)
BB1	120.4 (68.5)	7.2 (3.9)	1.5 (0.4)	5.8 (2.4)	0.7 (0.1)	1.1 (0.6)
BB2	428.7 (154.5)	22.0 (7.0)	0.6 (0.1)	18.6 (5.3)	1.2 (0.3)	4.8 (1.9)

[a]at 443 nm.
[b]$n = 29$.

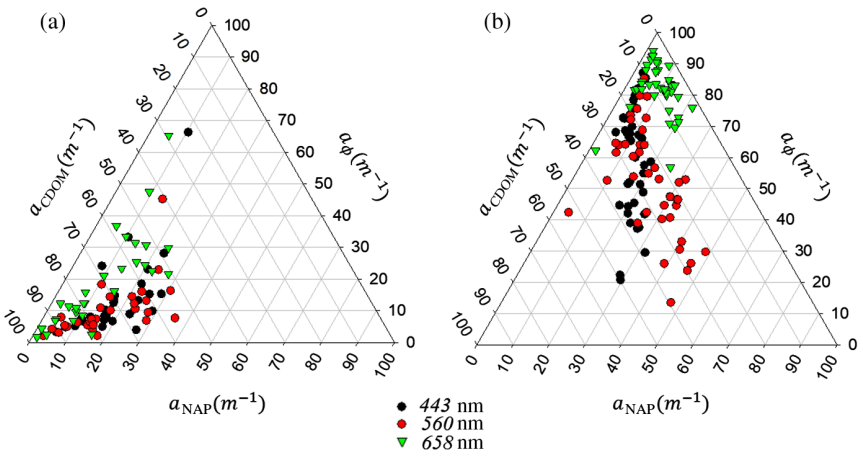

Fig. 2 Ternary plots depicting the relative contribution of a_{CDOM}, a_{NAP}, and a_{ϕ} from the total absorption except the water contribution for the wavelengths set at 443, 560, and 658 nm corresponding to (a) Ibi and (b) BB.

Table 3 Accuracy of the evaluated models for Z_{SD} estimation using QAA_{v5}, QAA_{M14}, and QAA_{W16} variants for IOPs derivation.

		BB	Ibi	All data
QAA_{v5}	RMSE (m)	0.49	0.89	0.69
	MAPE (%)	51.27	34.60	37.30
QAA_{M14}	RMSE (m)	0.42	0.87	0.65
	MAPE (%)	37.04	34.65	59.58
QAA_{W16}	RMSE (m)	0.35	1.03	0.72
	MAPE (%)	22.39	42.38	37.71

The Z_{SD} estimation for BB, which is dominated by phytoplankton, was improved when the IOPs were retrieved using QAA_{W16}, whereas for Ibi, which is an organic matter-dominated water, the QAA_{v5} version performed better than the others. Reference 16 also observed improvements on Z_{SD} estimation when the version of QAA_{v5} was modified. Reference 5 in order to derive K_d in a very turbid lake in Japan, evaluated a semianalytical approach. They noticed that replacing the QAA_{v5} by QAA_Turbid,[24] the retrieval of K_d had great improvements. Thus, the results corroborate to the fact that water bodies with different in-water composition can limit the application of a single approach to derive the IOPs, demanding for additional parameterization in order to achieve satisfactory outcomes.

The original model from Ref. 2 was validated using a wide range of data but very few from inland waters, and it showed an average absolute difference of 18% and R^2 of 0.96 with Z_{SD} ranging between <1 and >30 m without any additional reparameterization. In hypereutrophic to eutrophic waters such as BB, the estimation of a and b_b using QAA with $\lambda_0 = 560$ nm can be highly erroneous and according to Ref. 7, the a budget in such instances is dominated by nonwater constituents, which makes the empirical estimation of $a(560)$ weak. For very turbid productive waters, studies have shown that bands at longer wavelengths near 708 nm are suitable for IOPs estimation; however, this band is absent in Landsat-8.[7,8,24] The package effect can also be considered as a source of error influencing the absorption spectra by reducing it in places where the Chl-a exceeds 200 mg m^{-3},[25] leading to erroneous measures of R_{rs} (input for Z_{SD} modeling).

In case of Ibi, which is a CDOM-dominated system, the results revealed the suitability of QAA_{v5} in retrieving Z_{SD}. Reference 26 using different QAA forms, considering inland waters dominated by phytoplankton and coastal and sea waters, observed that QAA_{M14} and QAA_{v5}

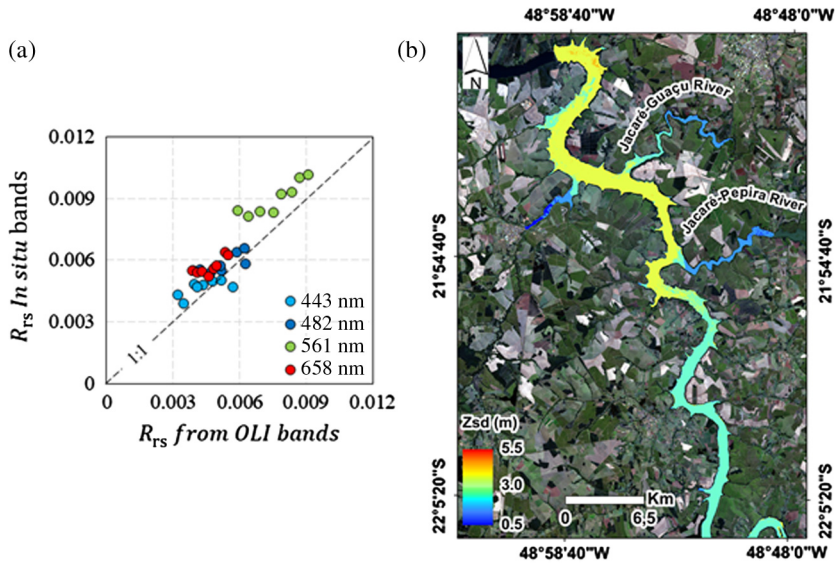

Fig. 3 Graphics showing the (a) validation between *in situ* R_{rs} and R_{rs} extracted from OLI image and (b) Z_{SD} analytically derived on OLI data.

returned better results, respectively, in CDOM-dominated reservoirs in Brazil. Mixing the steps from both algorithms and reparameterizing, the empirical step χ and the analytical step relative to $a(\lambda)$ retrieval by computing the CDOM influence, the results improved, and the normalized root mean square errors of a (400 to 750) were 30.71% and 14.51% for Funil and Itumbiara reservoirs, respectively. The modifications included OLCI bands.

The low Z_{SD} observed in BB was attributed to the presence of high concentrations of Chl-a and SPM. The relationships of Z_{SD} with Chl-a and SPM showed a nonlinear correlation ($R^2 = 0.72$ and $R^2 = 0.75$, respectively). In Ibi, the relationships of Z_{SD} with Chl-a and SPM also depicted a nonlinear correlation ($R^2 = 0.61$ and $R^2 = 0.60$, respectively). The biogeochemical analysis corroborated to these observations highlighting the high influence of phytoplankton on the water quality. High Chl-a is a direct result of high loads of nutrients that BB receives from urban centers and industries in the watershed. Ibi is the third reservoir in the cascade and due to its position along the river is still being influenced by the urban and industrial centers of the metropolitan region.

3.3 Z_{SD} Validation Using OLI Data

To evaluate the performance of the Z_{SD} model (based on QAA_{v5}) using satellite data, the bands simulated using *in situ* data were coanalyzed with OLI atmospherically corrected data acquired at the same day of sampling collection. The results showed an MAPE of 15.02%, 15.88%, 19.58%, and 22.37% correspondent to the bands centered at 443, 482, 560, and 658 nm, respectively [Fig. 3(a)]. After applying the Z_{SD} model based on QAA_{v5} on the OLI image from July 21, 2016 the results presented an RMSE of 0.46 m and MAPE of 19.04%.

According to Fig. 3(b), the water column from the south region showed increased attenuation than the north, and the same was also observed from the tributaries. These may be explained by the cascading reservoir continuum concept that demonstrate a growing eutrophication of the uppermost reservoirs, such as Bariri and BB placed upstream in the Tietê River, with an impact on the water quality of the downstream reservoirs.[27]

4 Conclusion

The semianalytical model from Ref. 2 was applied to two eutrophic reservoirs situated in the Tietê River. The results showed that Z_{SD} based on QAA_{W16} produced the lowest errors for BB and Z_{SD} based on QAA_{v5} yielded the lowest errors for Ibi. Both reservoirs have different

composition, and BB is dominated by phytoplankton, whereas Ibi is dominated by CDOM. These variability in bio-optical properties can lead to different performance of semianalytical approaches due to the presence of empirical steps in the modeling. The accuracy in BB was still not satisfactory most likely due to the package effect, which is a result of high concentrations of Chl-a. The Z_{SD} in BB showed an exponential decay with the SPM concentration ($R^2 = 0.72$) and a power function with Chl-a ($R^2 = 0.75$). The relationship among Z_{SD}, Chl-a, and SPM showed an inverse trend highlighting the decline of transparency with increasing suspended matter. In Ibi, Z_{SD} retrieved by QAA_{v5} and QAA_{M14} exhibited better results compared to other QAA version, but in order to be able to use Landsat-8 data, the first approach was picked. *In situ* Z_{SD} also had a nonlinear trend when correlated to Chl-a ($R^2 = 0.61$) and SPM ($R^2 = 0.60$) concentrations. The main issue in deriving Z_{SD} is the accurate determination of the IOPs, therefore, much effort is still needed to be undertaken in order to decrease the uncertainties in Z_{SD} modeling in aquatic systems varying widely in their optical properties.

Disclosures

No potential conflict of interest was reported by the authors.

Acknowledgments

The authors thank to FAPESP Projects (Process Nos. 2012/19821-1 and 2015/21586-9), Science without Borders/ CNPq Projects (400881/2013-6 and 472131/2012-5), and Coordination for the Improvement of Higher Education Personnel (CAPES) for scholarship.

References

1. H. Buiteveld, "A model for calculation of diffuse light attenuation (PAR) and Secchi depth," *Neth. J. Aquat. Ecol.* **29**(1), 55–65 (1995).
2. Z. P. Lee et al., "Secchi disk depth: a new theory and mechanistic model for underwater visibility," *Remote Sens. Environ.* **169**, 139–149 (2015).
3. K. Alikas and S. Kratzer, "Improved retrieval of Secchi depth for optically-complex waters using remote sensing data," *Ecol. Indic.* **77**, 218–227 (2017).
4. Z. Lee, K. L. Carder, and R. A. Arnone, "Deriving inherent optical properties from water color: a multiband quasi-analytical algorithm for optically deep waters," *Appl. Opt.* **41**(27), 5755–5772 (2002).
5. W. Yang et al., "Application of a semianalytical algorithm to remotely estimate diffuse attenuation coefficient in turbid inland waters," *IEEE Geosci. Remote Sens. Lett.* **11**(6), 1046–1050 (2014).
6. W. Yang et al., "A modified semianalytical algorithm for remotely estimating euphotic zone depth in turbid inland waters," *IEEE J. Sel. Top. Appl. Earth Obs. Remote Sens.* **8**(4), 1545–1554 (2015).
7. S. Mishra, D. R. Mishra, and Z. Lee, "Bio-optical inversion in highly turbid and cyanobacteria-dominated waters," *IEEE Trans. Geosci. Remote Sens.* **52**(1), 375–388 (2014).
8. F. Watanabe et al., "Parametrization and calibration of a quasi-analytical algorithm for tropical eutrophic waters," *ISPRS J. Photogramm. Remote Sens.* **121**, 28–47 (2016).
9. T. Rodrigues et al., "Estimating the optical properties of inorganic matter-dominated oligo-to-mesotrophic inland waters," *Water* **10**(449), 1–28 (2018).
10. Z. Lee et al., "An update of the quasi-analytical algorithm," 2009, http://www.ioccg.org/groups/Software_OCA/QAA_v5.pdf (10 June 2016).
11. AES Tietê, "Usinas e eclusas," 2015, http://ri.aestiete.com.br (14 June 2016).
12. M. J. Dellamano-Oliveira, V. Colombo-Corbi, and A. A. H. Vieira, "Dissolved carbohydrates from Barra Bonita Reservoir (São Paulo State, Brazil) and its relationships with phytoplanktonic abundant algae," *Biota Neotrop.* **7**(2), 59–66 (2007).
13. H. L. Golterman, R. S. Clymo, and M. A. M. Ohnstad, "Methods for physical and chemical analysis of fresh waters," in *IBP Handbook*, Vol. **8**, Blackwell Scientific Publications, Oxford (1978).

14. APHA, *Standard Methods for Examination of Water and Wastewater (Standard Methods for the Examination of Water and Wastewater)*, pp. 5–16, American Public Health Association, New York (1998).
15. C. D. Mobley, "Estimation of the remote-sensing reflectance from above-surface measurements," *Appl. Opt.* **38**(36), 7442–7455 (1999).
16. Z. Lee et al., "Removal of surface-reflected light for the measurement of remote-sensing reflectance from an above-surface platform," *Opt. Express* **18**(25), 26313–26324 (2010).
17. T. Rodrigues et al., "Retrieval of Secchi disk depth from a reservoir using a semi-analytical scheme," *Remote Sens. Environ.* **198**, 213–228 (2017).
18. H. R. Gordon, "Remote sensing of ocean color: a methodology for dealing with broad spectral bands and significant out-of-band response," *Appl. Opt.* **34**(36), 8363–8374 (1995).
19. J. A. Barsi et al., "The spectral response of the Landsat-8 operational land imager," *Remote Sens.* **6**(10), 10232–10251 (2014).
20. C. Pelloquin and J. Nieke, "SENTINEL-3 spectral response functions for optical instruments (version CDR)," Technical Note, 2012, European Space Agency, https://earth.esa.int/web/guest/home (26 September 2012).
21. J. A. Concha and J. R. Schott, "Retrieval of color producing agents in Case 2 waters using Landsat 8," *Remote Sens. Environ.* **185**, 95–107 (2016).
22. F. S. Y. Watanabe et al., "Drought can cause phytoplankton growth intensification in Barra Bonita reservoir," *Model. Earth Syst. Environ.* **2**(3), 134 (2016).
23. C. T. Cairo et al., "Spatial and seasonal variation in diffuse attenuation coefficients of downward irradiance at Ibitinga Reservoir, São Paulo, Brazil," *Hydrobiologia* **784**(1), 265–282 (2017).
24. W. Yang et al., "Retrieval of inherent optical properties for turbid inland waters from remote-sensing reflectance," *IEEE Trans. Geosci. Remote Sens.* **51**(6), 3761–3773 (2013).
25. E. Alcântara et al., "An investigation into the phytoplankton package effect on the chlorophyll-a specific absorption coefficient in Barra Bonita reservoir, Brazil," *Remote Sens. Lett.* **7**(8), 761–770 (2016).
26. I. Ogashawara et al., "Re-parameterization of a quasi-analytical algorithm for colored dissolved organic matter dominant inland waters," *Int. J. Appl. Earth Obs. Geoinf.* **53**, 128–145 (2016).
27. F. A. R. Barbosa et al., "The cascading reservoir continuum concept (CRCC) and its application to the river Tietê-basin, São Paulo State, Brazil," in *Workshop on Theoretical Reservoir Ecology and Its Applications*, pp. 425–437 (1999).

Thanan Rodrigues received her BS degree in agronomy from the Amazon Federal University in 2006, MS degree in geology from Pará Federal University, Brazil, in 2009 and PhD in cartographic science from the São Paulo State University (UNESP—University Estadual Paulista) in 2017. Currently, she is a professor in Federal Institute of Pará State (IFPA).

Enner Alcântara received his BS degree in aquatic sciences from the Federal University of Maranhão in 2005 and his PhD in remote sensing from the Brazilian Institute for Space Research in 2010. Currently, he is an assistant professor in São Paulo State University (UNESP—University Estadual Paulista).

Deepak R. Mishra received his PhD in natural resources from the University of Nebraska, Lincoln, in 2006. Currently, he is an associate professor of geography at the University of Georgia, where he operates the Remote Sensing and Spectroscopy Laboratory (RSSL) and Small Satellite Research Laboratory (SSRL). Over the past few years, most of his research efforts have been devoted to the development of spectral models and geospatial techniques for monitoring freshwater and shallow marine ecosystems.

Fernanda Watanabe received her BS degree in environmental engineering from the São Paulo State University in 2009 and the PhD in cartographic science from the São Paulo State University (UNESP—University Estadual Paulista), Brazil, in 2016. She is an assistant professor in the Department of Cartography, São Paulo State University. Her research interests are specially

in remote sensing of water color, bio-optical modeling, and monitoring and mapping of water quality in inland waters.

Nariane Bernardo received her BS degree in environmental engineering from the Federal University of Technology, Paraná (UTFPR) and master's degree in cartographic sciences from the São Paulo State University in 2015. Currently, she is a PhD student in São Paulo State University (UNESP—Univ. Estadual Paulista).

Luiz Rotta received his BS degree in environmental engineering in 2008 and received his PhD in cartographic science from the São Paulo State University (UNESP—University Estadual Paulista), Brazil, in 2015. He is postdoctoral researcher in the Department of Cartography, São Paulo State University. His research interests include water quality remote sensing of inland waters, submerged aquatic vegetation mapping, and bio-optical modeling.

Nilton Imai received his BS degree in agricultural engineering from the State University of Campinas in 1979, master's degree in remote sensing by the National Institute for Space Research in 1986 and his doctorate in geography (human geography) from the University of São Paulo in 1996. Currently, he is an assistant professor at São Paulo State University (UNESP—University Estadual Paulista), Department of Cartography. He has experience in geosciences, remote sensing, mainly in remote sensing and GIS.

Ike Astuti is an assistant professor (Asisten Ahli) at the Department of Geography, State University of Malang, Indonesia. She obtained her BS (Sarjana) in soil science, Bogor Agricultural University (Institut Pertanian Bogor), received a master's degree in natural resource studies from the University of Queensland, Australia, and received her PhD in geography from the Department of Geography, University of Georgia in 2017. Her research interest includes application of remote sensing for landscape monitoring and water resources.